DIRECT AND LARGE EDDY SIMULATION OF STRATIFIED TURBULENCE

Sebastian Remmler
Institute of Aerodynamics and Fluid Mechanics, Technische Universität München
85747 Garching bei München, Germany
remmler@tum.de

Stefan Hickel
Institute of Aerodynamics and Fluid Mechanics, Technische Universität München
sh@tum.de

ABSTRACT

Simulation of geophysical turbulent flows requires a robust and accurate subgrid-scale turbulence modeling. We propose an implicit subgrid-scale model for stratified fluids, based on the Adaptive Local Deconvolution Method. To validate this turbulence model, we performed direct numerical simulations of the transition of the three-dimensional Taylor–Green vortex and homogeneous stratified turbulence. Our analysis proves that the implicit turbulence model correctly predicts the turbulence energy budget and the spectral structure of stratified turbulence.

INTRODUCTION

Turbulence in fluids is strongly affected by the presence of density stratification which is a common situation in geophysical flows. To predict atmospheric and oceanic mesoscale flows, we need to understand and parametrize the small scale turbulence. The stratification suppresses vertical motions and thus makes all scales of the velocity field strongly anisotropic. The horizontal velocity spectrum in the atmosphere was analyzed by Nastrom & Gage (1985) using aircraft observations. They found a power-law behavior in the mesoscale range with an exponent of -5/3. In the vertical spectrum, on the other hand, Cot (2001) observed an exponent of -3 in the inertial range.

There has been a long an intensive discussion whether the observed spectra are due to a backward cascade of energy (Gage, 1979; Lilly, 1983; Herring & Métais, 1989) as in two-dimensional turbulence (Kraichnan, 1967), or due to breaking of internal waves, which means that a forward cascade is the dominant process (Dewan, 1979; van Zandt, 1982). In different numerical and theoretical studies, ambiguous or even conflicting results were obtained (Lilly *et al.*, 1998).

During the last decade, a number of new simulations and experiments addressed the issue. Smith & Waleffe (2002) observed a concentration of energy in the lowest modes in their simulations. Other studies (Laval *et al.*, 2003; Waite & Bartello, 2004) suggested that the character of the flow depends on the Reynolds number. Apparently, high Reynolds numbers are associated with stronger three-dimensionality and a forward cascade of energy. Lindborg (2006) presented a scaling analysis of the Boussinesq equations for low Froude and high Reynolds number. His theory of strongly anisotropic, but still three-dimensional, turbulence explains the horizontal $k_h^{-5/3}$-spectrum as well as the vertical k_v^{-3}-spectrum. On the basis of these findings, Brethouwer *et al.* (2007) showed that the relevant non-dimensional parameter controlling stratified turbulence is the buoyancy Reynolds number $\mathscr{R} = \mathrm{Fr}^2\mathrm{Re}$. For $\mathscr{R} \gg 1$, they predict stratified turbulence including local overturning and a forward energy cascade. In the opposite limit, for $\mathscr{R} \ll 1$, the flow is controlled by viscosity and does not contain small-scale turbulent motions.

Since a full resolution of all turbulence scales is only possible for very low Reynolds numbers, many groups used subgrid-scale (SGS) models in their computations. E. g., Métais & Lesieur (1992) used a spectral eddy viscosity model, based on the eddy damped quasi-normal Markovian (EDQNM) theory. This required a flow simulation in Fourier space and the cut-off wavenumber to be in the inertial range. For classical large eddy simulations (LES) in physical space, Smagorinsky models are widely used, either in the classical formulation (Kaltenbach *et al.*, 1994) or with certain modifications for stratified turbulence based in the local Richardson number (Dörnbrack, 1998). Staquet & Godeferd (1998) presented a two-point closure statistical EDQNM turbulence model, which was adapted for axisymmetric spectra about the vertical axis. Recently, many groups presented regularized direct numerical simulations (DNS) of stratified turbulence, which means rather pragmatically stabilizing under-resolved DNS by removing the smallest resolved scales. This is obtained by a hyperviscosity approach (Lindborg, 2006) or by de-aliasing in spectral methods using the “2/3-rule” (Bouruet-Aubertot *et al.*, 1996; Fritts *et al.*, 2009).

All SGS turbulence models suffer from the problem that the computed SGS stresses are of the same order as the grid truncation error. This typically leads to interference between

SGS model and numerical scheme, instability and worse results on refined grids. This issue can be solved by combining discretization scheme and SGS model in a single approach. This is usually referred to as "implicit" LES (ILES) in contrast to the traditional "explicit" SGS models. The idea of ILES was realized by Hickel *et al.* (2006) in the Adaptive Local Deconvolution Method (ALDM) for neutrally stratified fluids. Based on this method and ALDM for passive scalar transport (Hickel *et al.*, 2007), we developed an implicit SGS model for Boussinesq fluids. In the present paper, we will evaluate the applicability of ALDM for stably stratified turbulence.

We simulated transition and decay of the three-dimensional Tailor–Green vortex as an example of a transitional stratified turbulent flow. For isotropic conditions, this flow was intensively studied by Brachet *et al.* (1983). Riley & de Bruyn Kops (2003) first simulated its evolution in a stably stratified background. The second test case to be covered is forced homogeneous stratified turbulence at different Froude and Reynolds numbers. For both cases, we present not only ILES, but also LES with a standard Smagorinsky model (SSM) and high-resolution DNS as benchmark solutions.

GOVERNING EQUATIONS

The non-dimensional Boussinesq equations for a stably stratified fluid in Cartesian coordinates read

$$\nabla \cdot \mathbf{u} = 0 \tag{1a}$$

$$\partial_t \mathbf{u} + \nabla \cdot (\mathbf{u}\mathbf{u}) = -\nabla p - \frac{\rho}{\mathrm{Fr}_0^2}\mathbf{e}_z + \frac{1}{\mathrm{Re}_0}\nabla^2 \mathbf{u} \tag{1b}$$

$$\partial_t \rho + \nabla \cdot (\rho \mathbf{u}) = -w + \frac{1}{\mathrm{Pr}\,\mathrm{Re}_0}\nabla^2 \rho \tag{1c}$$

where velocities are made non-dimensional by $\mathscr{U}$, all spatial coordinates by the length scale $\mathscr{L}$, pressure by $\mathscr{U}^2$, time by $\mathscr{L}/\mathscr{U}$, and density fluctuation $\rho = \rho^* - \overline{\rho}$ (ρ^*: local absolute density, $\overline{\rho}$: background density) by the background density gradient $\mathscr{L}|d\overline{\rho}/dz|$. The non-dimensional parameters are

$$\mathrm{Fr}_0 = \frac{\mathscr{U}}{N\mathscr{L}}\ , \quad \mathrm{Re}_0 = \frac{\mathscr{U}\mathscr{L}}{\nu}\ , \quad \mathrm{Pr} = \frac{\nu}{\mu} \tag{2}$$

We chose a Prandtl number of Pr = 0.7, corresponding to values found in the atmosphere. Froude and Reynolds number are used as parameters to control the flow regime.

With the instantaneous values of kinetic energy E_k and kinetic energy dissipation ε_k, we find the local Froude and Reynolds number as well as the buoyancy Reynolds number $\mathscr{R}$, defined by Brethouwer *et al.* (2007):

$$\mathrm{Fr} = \frac{\mathrm{Fr}_0 \mathscr{L}}{\mathscr{U}}\frac{\varepsilon_k}{E_k}\ , \quad \mathrm{Re} = \frac{\mathrm{Re}_0}{\mathscr{U}\mathscr{L}}\frac{E_k^2}{\varepsilon_k}\ , \quad \mathscr{R} = \mathrm{Re}\,\mathrm{Fr}^2 \tag{3}$$

In ILES by construction we do not have direct access to the value of ε_k. We thus computed it from the total dissipation rate, assuming a constant mixing ratio of $\varepsilon_p/\varepsilon_k = 0.4$, which is an acceptable approximation for a wide range of parameters.

NUMERICAL METHOD

We extended our existing finite-volume solver INCA for isothermal incompressible Navier-Stokes equations with scalar transport to solve the Boussinesq equations by adding the corresponding source terms in the equations for transport of vertical momentum and buoyancy.

All computations were run on Cartesian staggered grids with uniform cell size. The code offers different discretization schemes depending on the application. For DNS and LES with SSM, we used a non-dissipative central difference scheme with 4$^{\text{th}}$ order accuracy for the convective terms and 2$^{\text{nd}}$ order central differences for the diffusive terms and the continuity equation (Poisson equation for pressure).

For implicit LES, we replaced the central difference scheme for the convective terms by the implicit turbulence model ALDM. The method is based on a reconstruction of the unfiltered solution on the represented scales by combining Harten-type deconvolution polynomials. The different polynomials are dynamically weighted based on the smoothness of the filtered solution. A tailored numerical flux function operates on the approximately reconstructed solution. Both, the solution-adaptive polynomial weighting and the numerical flux function involve free model parameters, that were calibrated in such a way that the truncation error of the discretized equations correctly represents the SGS stresses of turbulence (Hickel *et al.*, 2006). This set of parameters was not changed for any subsequent applications of ALDM. For the presented computations, we used an implementation of ALDM with improved computational efficiency. The validity of this method has been proved for a number of applications (e. g. Hickel *et al.*, 2008).

For time integration, we used an explicit third-order accurate Runge-Kutta scheme, as proposed by Shu (1988). The time step was dynamically adjusted to keep the CFL number smaller than unity.

TEST CASES AND RESULTS

Taylor–Green Vortex (TGV)

Transitional flows impose a special problem to turbulence subgrid-scale models. Their correct prediction is only possible if the subgrid-scale model does not affect the laminar flow and its instability modes. For most eddy-viscosity models, such as the Smagorinsky model, this requirement is not fulfilled. We used the transition of the three-dimensional Taylor–Green vortex (TGV) as a test for ALDM in laminar-to-turbulence transition. The flow field in a triple-periodic box with side length $L_D = 2\pi\mathscr{L}$ is initialized with a set of large scale vortices varying vertically:

$$\mathbf{u} = \mathscr{U}\cos(z/\mathscr{L})\begin{bmatrix}\cos(x/\mathscr{L})\sin(y/\mathscr{L})\\ -\sin(x/\mathscr{L})\cos(y/\mathscr{L})\\ 0\end{bmatrix} \tag{4}$$

where $\mathscr{U}$ and $\mathscr{L}$ are characteristic velocity and length scales of the problem.

Initially, all flow energy is concentrated on the lowest wavenumbers. The flow is purely horizontal, laminar and strongly anisotropic. At later times, energy is transferred to smaller scales by vortex stretching. After approximately 10

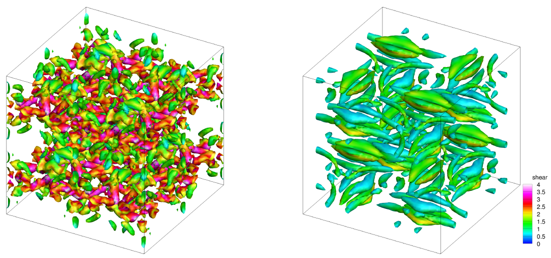

(a) neutral stratification (b) stable stratification, $\mathrm{Fr}_0 = 1$

Figure 1. Visualization of the TGV at $t = 10$ ($\mathrm{Re}_0 = 1600$). Iso-surfaces at $Q = 0.5$, colored by the shear rate.

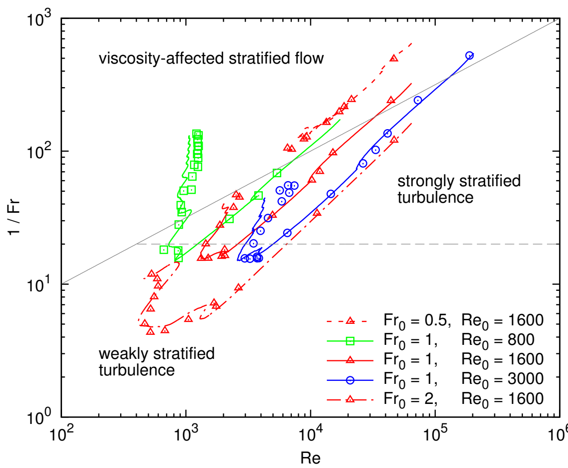

Figure 2. Regime diagram (Brethouwer *et al.*, 2007) for the transition of the TGV for different parameters; symbols: DNS, lines: LES with ALDM

non-dimensional time units, the flow is quasi-turbulent, keeping its determinism and spatial symmetry. At this time, the energy dissipation has a maximum due to the enhanced shear in the small scale vortices. If neutrally stratified, the energy of the vertical velocity component soon reaches the level of the horizontal components and the flow gets isotropic. I case of a stable background stratification, vertical motions are damped by the restoring buoyancy force and the flow remains highly anisotropic. In the linear limit of zero Froude number, the stratification completely prevents the transition to turbulence.

For DNS, the number of computational cells depends on the Reynolds number. We used 256^3 cells for $\mathrm{Re}_0 = 800$, 512^3 cells for $\mathrm{Re}_0 = 1600$, and 768^3 cells for $\mathrm{Re}_0 = 3000$, to be sure to resolve the smallest turbulence scales. With LES, the resolution is Reynolds number independent. We used 64^3 cells for all LES.

The effect of a density stratification on turbulence is illustrated in fig. 1, which shows a visualization of the turbulence structures approximately at the time of maximum dissipation. In a stratified medium, the coherent structures are larger and anisotropic and the shear rate magnitude is lower compared to neutral stratification.

The local Froude and Reynolds number in the TGV flow field are rapidly changing during the transition. To verify that the transition occurs in a relevant parameter space, we show

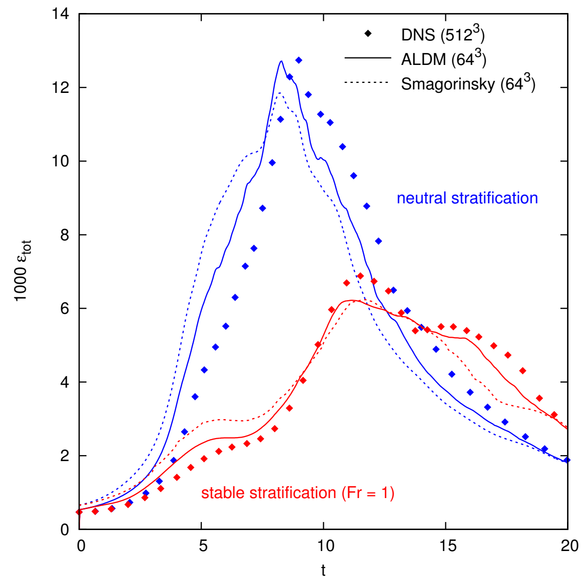

Figure 3. Total energy dissipation rate of the TGV ($\mathrm{Re}_0 = 1600$)

the tracks of several TGV simulations in fig. 2. Indeed, most of the simulations are located in the regime of stratified turbulence. Hence they are suitable for validation of a SGS model for stratified turbulence.

An LES must be able to correctly predict the temporal evolution of the total dissipation rate by modeling the effect of the small scale vortices on the larger scales. In fig. 3, we show the results from LES on a 64^3 cell grid using ALDM as well as the SSM compared to a DNS on a grid with 512^3 cells. For neutral and moderately stable stratification, the ALDM yields better results than the SSM. For neutral stratification, Hickel *et al.* (2006) compared ALDM to a dynamic Smagorinsky model and the spectral eddy viscosity model of Chollet & Lesieur (1981). They found better agreement of the LES solution with DNS data if ALDM was used, compared to both alternative parametrizations.

In figures 4 to 6, we show the contributions of molecular and implicit SGS dissipation to the total dissipation in LES with ALDM for three different intensities of stratification. The relative amount of implicit SGS dissipation decreases with increasing stratification, since the flow is better resolved in cases of strong stratification. For $\mathrm{Fr}_0 = 2$ and $\mathrm{Fr}_0 = 1$, the dissipation peaks are dominated by implicit SGS dissipation, which shows that the implicit model is automatically activated, when it is needed, and provides a good approximation of the unresolved stresses for different intensities of stratification.

The ratios of the different types of energy in the TGV vary constantly during the evolution. While initially there is only horizontal kinetic energy, at later times a certain fraction of this energy is converted to vertical kinetic energy as well as available potential energy. The energy budget for one representative case is shown in fig. 7. Both LES, with implicit ALDM and with explicit SSM, predict the energy conversions with good accuracy. The best agreement is obtained for the horizontal kinetic energy component. The overall agreement

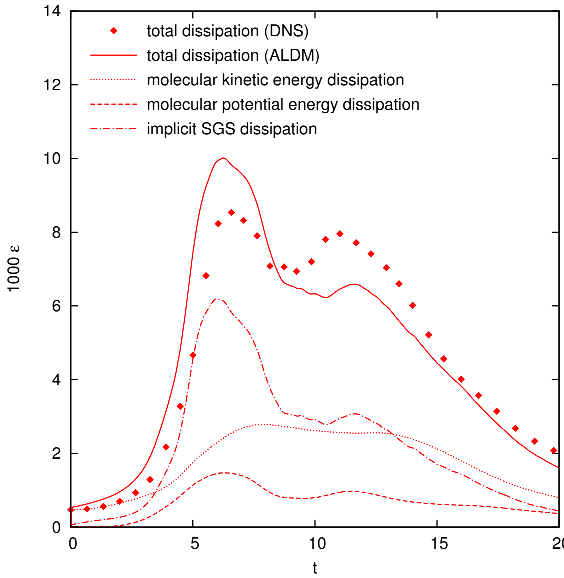

Figure 4. Contributions to energy dissipation of the TGV ($\mathrm{Re}_0 = 1600$, $\mathrm{Fr}_0 = 2$)

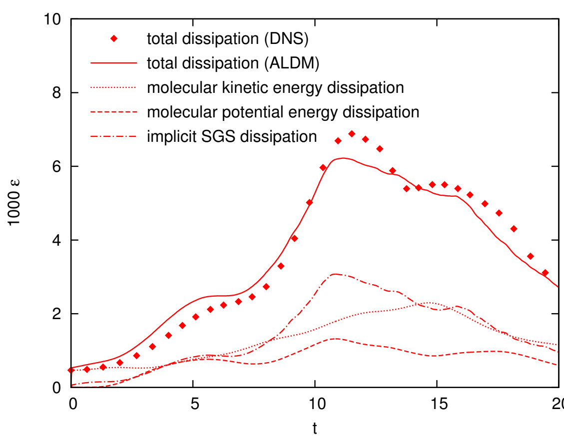

Figure 5. Contributions to energy dissipation of the TGV ($\mathrm{Re}_0 = 1600$, $\mathrm{Fr}_0 = 1$)

with DNS data is better if ALDM is used.

Homogeneous Stratified Turbulence (HST)

The second investigated test case is homogeneous stratified turbulence in a statistically steady state. The flow is maintained at an approximately constant energy level by a large scale vertically uniform forcing of the horizontal velocity components. This approach was successfully applied by several authors before (Métais & Herring, 1989; Waite & Bartello, 2004; Lindborg, 2006).

We ran two series of DNS, series A with $\mathrm{Re}_0 = 6500$ and series B with $\mathrm{Re}_0 = 13\,000$. The domain size was 320^3 cells for series A and 640^3 cells for series B. Within the single series, the Froude number was varied to cover different buoyancy Reynolds numbers. The basic domain size again was $2\pi\mathscr{L}$. For low Froude numbers, we used a flat domain with a height of only $\pi\mathscr{L}$, but keeping cubical cells. This is permitted since in stratified turbulence there is only a very small amount of energy contained in the low vertical modes.

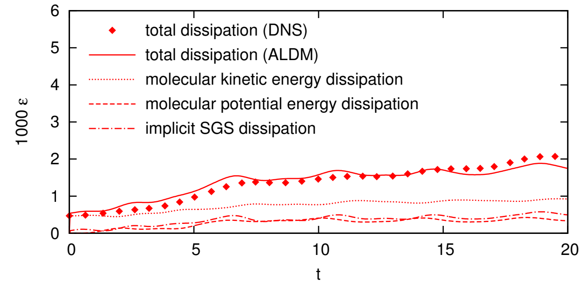

Figure 6. Contributions to energy dissipation of the TGV ($\mathrm{Re}_0 = 1600$, $\mathrm{Fr}_0 = 0.5$)

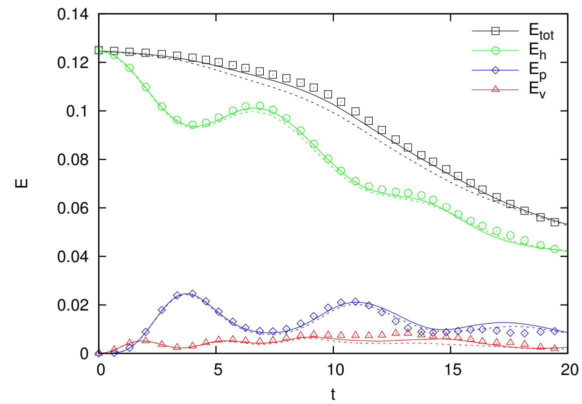

Figure 7. Energy budget of the TGV ($\mathrm{Re}_0 = 1600$, $\mathrm{Fr}_0 = 1$); solid lines: ALDM, dashed lines: SSM

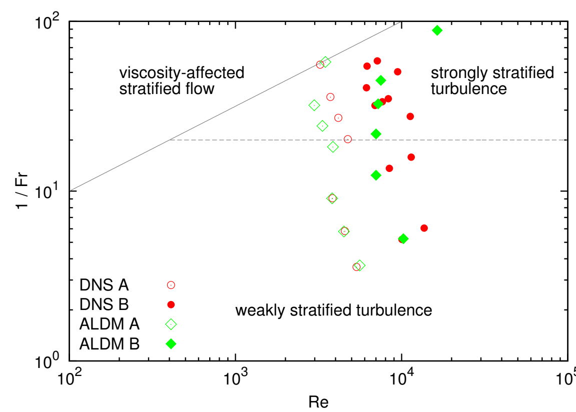

Figure 8. Regime diagram for our simulations of stratified turbulence

For both series, we performed LES, both with implicit ALDM and explicit SSM. For all these, we used grid boxes with 64^3 cells. For the low Froude number simulations, the domain was flattened as well, leading to a doubled resolution in vertical direction. Fig. 8 shows the local Froude and Reynolds number of the single simulations.

Most important for the assessment of a parametrization scheme for stratified turbulence is its ability to correctly pre-

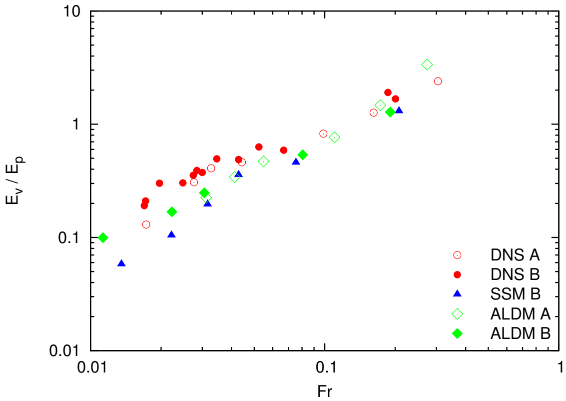

Figure 9. Ratio of vertical to potential energy in HST as a function of local Froude number

dict the amount of energy converted from horizontal kinetic energy to vertical kinetic energy and available potential energy before the energy is finally dissipated on the smallest represented scales. In fig. 9, we show the ratio E_v/E_p as a function of local Froude number as predicted by DNS and LES with ALDM. The ratio E_v/E_p cannot be influenced by the forcing and can thus freely develop only due to the interaction of convective, pressure and buoyancy term.

The vertical to potential energy ratio increases almost linearly with Froude number in the DNS. We find the same trend in our LES with ALDM. The agreement between DNS and LES is best in the region of high Froude numbers (weakly stratified turbulence), whereas for low Froude numbers, the vertical kinetic energy is slightly underpredicted. Note that the difference between results from ALDM and SSM differ from each other most at the lowest Froude number. This is an indication for ALDM being better capable of handling the strong turbulence anisotropy in strongly stratified flows.

For comparison of kinetic energy spectra in fig. 10, we selected one DNS in the strongly stratified regime ($\mathscr{R}$ = 6.3, Fr = 0.03, Re = 8300) and one DNS in the weakly stratified regime ($\mathscr{R}$ = 41, Fr = 0.07, Re = 9300), both from series B. The corresponding LES have similar local Froude and Reynolds numbers.

In the horizontal spectra of kinetic energy, the difference between ALDM and a simple eddy viscosity model is most obvious. In the weakly stratified case ($\mathscr{R}$ = 41), the horizontal spectrum is still quite similar to the Kolmogorov spectrum of isotropic turbulence. In this case, both SGS models predict the inertial range spectrum fairly well. The SSM is slightly too dissipative, but the difference to the DNS spectrum is acceptable. Things completely change for the stronger stratified case ($\mathscr{R}$ = 6.3). The SSM dissipates too much energy and thus underpredicts the inertial range spectrum by more than one order of magnitude. Additionally, the predicted power-law exponent is significantly lower than -5/3. The spectrum predicted by ALDM, on the other hand, agrees well with the DNS. It correctly predicts the characteristic plateau region between the forcing scales and the inertial scales. Moreover, it produces a power-law decay with an exponent of -5/3, corresponding to the DNS and theory derived from scaling laws (Brethouwer *et al.*, 2007).

In the vertical spectra of kinetic energy, the inertial range decay exponent changes from -5/3 in neutrally stratified fluid to -3 in strongly stratified turbulence. We find this change in the DNS and it is well reproduced by the LES. Both SGS models predict the turbulence inertial range decay well. At strong stratification, the ALDM result perfectly agrees with the DNS. The SSM result is slightly too dissipative in this region.

CONCLUSION

We presented a numerical investigation of turbulence in a stably stratified fluid to proof the reliability of implicit turbulence modeling with the Adaptive Local Deconvolution Method (ALDM). As benchmark results, we used high resolution DNS data and LES results with an explicit Smagorinsky model. The investigated test cases were the transition of the three-dimensional Taylor–Green vortex (TGV) and horizontally forced homogeneous stratified turbulence (HST). In most simulations, the buoyancy Reynolds number was larger than unity. The Froude and Reynolds number were chosen to cover the complete range from isotropic Kolmogorov turbulence up to strongly stratified turbulence.

For the transition of the TGV, we found good agreement between ALDM results and DNS in neutrally and stably stratified fluid. With the implicit model, we generally obtained better results than with a SSM. This demonstrates the ability of ALDM to properly represent the SGS stresses in a transitional stratified flow. In HST, the ALDM results also agree well with the reference DNS, both in integral flow properties and energy spectra. This applies for the whole Froude number range from infinity down to very low values. Especially in the strongly stratified regime, the superiority of ALDM over the SSM is striking. While the SSM is far too dissipative in this case, ALDM spectra agree very well with the reference DNS.

The results presented here were obtained without recalibrating the ALDM model constants for stratified turbulence. The good agreement with DNS data shows the ability of ALDM to automatically adapt to strongly anisotropic turbulence. Within the continuation of the project, we will investigate to which extend the results can be further improved by a recalibration of the model coefficients for stratified turbulence. But even without this possible improvements, we can use ALDM as a reliable turbulence SGS model for geophysical applications.

ACKNOWLEDGMENTS This work was funded by the German Research Foundation (DFG) in line of the MetStröm priority program. Computational resources were provided by the High Performance Computing Center Stuttgart (HLRS).

REFERENCES

Bouruet-Aubertot, P., Sommeria, J. & Staquet, C. 1996 Stratified turbulence produced by internal wave breaking: two-dimensional numerical experiments. *Dyn. Atmos. Oceans* **23** (1-4), 357 – 369, stratified flows.

Brachet, M. E., Meiron, D., Orszag, S., Nickel, B., Morf, R. & Frisch, U. 1983 Small-scale structure of the Taylor–Green vortex. *J. Fluid Mech.* **130**, 411–452.

Brethouwer, G., Billant, P., Lindborg, E. & Chomaz, J.-M. 2007 Scaling analysis and simulation of strongly stratified turbulent flows. *J. Fluid Mech.* **585**, 343–368.

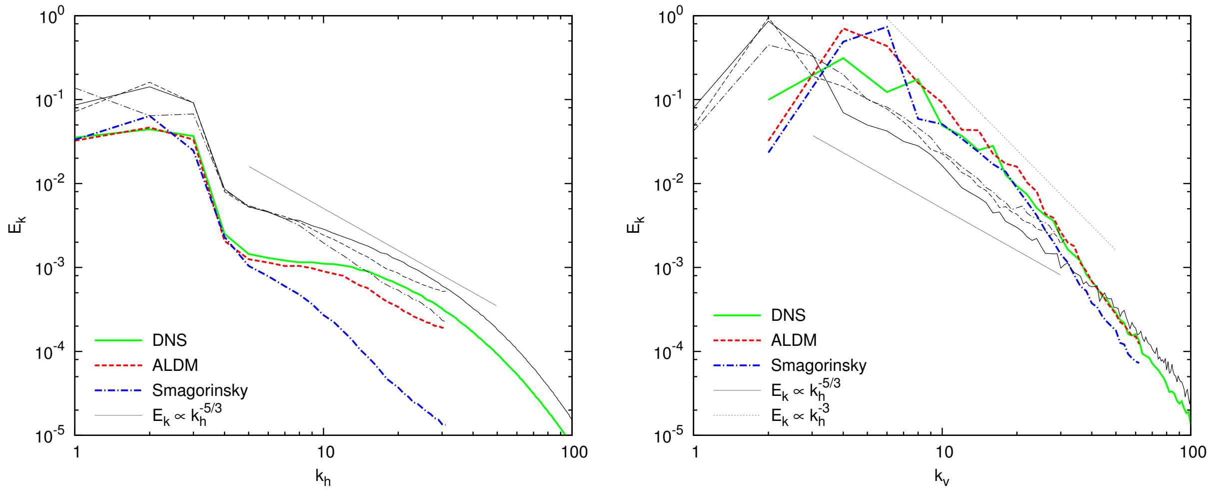

(a) Horizontal spectra

(b) Vertical spectra

Figure 10. Stratified turbulence kinetic energy spectra; thick colored lines: $\mathscr{R} = 6.3$, thin black lines: $\mathscr{R} = 41$

Chollet, J.-P. & Lesieur, M. 1981 Parameterization of small scales of three-dimensional isotropic turbulence utilizing spectral closures. *Journal of the Atmospheric Sciences* **38** (12), 2747–2757.

Cot, C. 2001 Equatorial mesoscale wind and temperature fluctuations in the lower atmosphere. *J. Geophys. Res.* **106(D2)**, 1523–1532.

Dewan, Edmond M. 1979 Stratospheric wave spectra resembling turbulence. *Science* **204** (4395), 832–835.

Dörnbrack, A. 1998 Turbulent mixing by breaking gravity waves. *J. Fluid Mech.* **375**, 113–141.

Fritts, David C., Wang, Ling, Werne, Joe, Lund, Tom & Wan, Kam 2009 Gravity wave instability dynamics at high reynolds numbers. part i: Wave field evolution at large amplitudes and high frequencies. *J. Atmos. Sci.* **66** (5), 1126–1148.

Gage, K. S. 1979 Evidence for a $k^{-5/3}$ law inertial range in mesoscale two-dimensional turbulence. *J. Atmos. Sci.* **36**, 1950–1954.

Herring, Jackson R. & Métais, Olivier 1989 Numerical experiments in forced stably stratified turbulence. *J. Fluid Mech.* **202(1)**, 97–115.

Hickel, S., Adams, N. A. & Domaradzki, J. A. 2006 An adaptive local deconvolution method for implicit LES. *J. Comput. Phys.* **213**, 413–436.

Hickel, S., Adams, N. A. & Mansour, N. N. 2007 Implicit subgrid-scale modeling for large-eddy simulation of passive scalar mixing. *Phys. Fluids* **19**, 095102.

Hickel, S., Kempe, T. & Adams, N. A. 2008 Implicit large-eddy simulation applied to turbulent channel flow with periodic constrictions. *Theor. Comput. Fluid Dyn.* **22**, 227–242.

Kaltenbach, H.-J., Gerz, T. & Schumann, U. 1994 Large-eddy simulation of homogeneous turbulence and diffusion in stably stratified shear flow. *J. Fluid Mech.* **280** (1), 1–40.

Kraichnan, Robert H. 1967 Inertial ranges in two-dimensional turbulence. *Phys. Fluids* **10** (7), 1417–1423.

Laval, J.-P., McWilliams, J. C. & Dubrulle, B. 2003 Forced stratified turbulence: Successive transitions with Reynolds number. *Phys. Rev. E* **68** (3), 036308.

Lilly, D. K. 1983 Stratified turbulence and the mesoscale variability of the atmosphere. *J. Atmos. Sci.* **40** (3), 749–761.

Lilly, Douglas K., Bassett, Gene, Droegemeier, Kelvin & Bartello, Peter 1998 Stratified turbulence in the atmospheric mesoscales. *Theor. Comput. Fluid Dyn.* **11**, 139–153, 10.1007/s001620050085.

Lindborg, Erik 2006 The energy cascade in a strongly stratified fluid. *J. Fluid Mech.* **550** (1), 207–242.

Métais, Olivier & Herring, Jackson R. 1989 Numerical simulations of freely evolving turbulence in stably stratified fluids. *J. Fluid Mech.* **202** (1), 117–148.

Métais, Olivier & Lesieur, Marcel 1992 Spectral large-eddy simulation of isotropic and stably stratified turbulence. *J. Fluid Mech.* **239**, 157–194.

Nastrom, G. D. & Gage, K. S. 1985 A climatology of atmospheric wavenumber spectra of wind and temperature observed by commercial aircraft. *J. Atmos. Sci.* **42** (9), 950–960.

Riley, J. J. & de Bruyn Kops, S. M. 2003 Dynamics of turbulence strongly influenced by buoyancy. *Phys. Fluids* **15(7)**, 2047–2059.

Shu, C.-W. 1988 Total-variation-diminishing time discretizations. *SIAM J. Sci. Stat. Comput.* **9(6)**, 1073–1084.

Smith, LESLIE M. & Waleffe, FABIAN 2002 Generation of slow large scales in forced rotating stratified turbulence. *J. Fluid Mech.* **451** (1), 145–168.

Staquet, C. & Godeferd, F. S. 1998 Statistical modelling and direct numerical simulations of decaying stably stratified turbulence. Part 1. Flow energetics. *J. Fluid Mech.* **360**, 295–340.

van Zandt, T. E. 1982 A universal spectrum of buoyancy waves in the atmosphere. *Geophys. Res. Lett.* **9** (5), 575–578.

Waite, M. L. & Bartello, P. 2004 Stratified turbulence dominated by vortical motion. *J. Fluid Mech.* **517**, 281–308.